ZooKeys 108: 73–97 (2011)
doi: 10.3897/zookeys.108.1129
www.zookeys.org

RESEARCH ARTICLE

A peer-reviewed open-access journal
ZooKeys
Launched to accelerate biodiversity research

A new species of Andean toad (Bufonidae, *Osornophryne*) discovered using molecular and morphological data, with a taxonomic key for the genus

Diego J. Páez-Moscoso[1,†], Juan M. Guayasamin[2,‡], Mario Yánez-Muñoz[1,3,4,§]

1 *Museo de Zoología, Escuela de Ciencias Biológicas, Pontificia Universidad Católica del Ecuador, Av. 12 de Octubre y Roca, Aptdo. 17-01-2184, Quito, Ecuador* **2** *Centro de Investigación de la Biodiversidad y el Cambio Climático, Universidad Tecnológica Indoamérica, Av. Machala y Sabanilla, Quito, Ecuador* **3** *División de Herpetología, Museo Ecuatoriano de Ciencias Naturales, Rumipamba 341 y Av. de los Shyris. Quito, Ecuador* **4** *Programa de Maestría en Biología de la Conservación, Pontificia Universidad Católica del Ecuador. Av. 12 de Octubre y Roca, Aptdo. 17-01-2184, Quito, Ecuador*

† *urn:lsid:zoobank.org:author:C7E6B7EF-65B3-4083-9DBF-B11E9FFE8485*
‡ *urn:lsid:zoobank.org:author:73FF62CF-DA13-46D3-95FB-E0B7208AA6E7*
§ *urn:lsid:zoobank.org:author:4F85DEF3-9AA1-4621-8566-1FE501361DA5*

Corresponding author: *Juan M. Guayasamin* (jmguayasamin@gmail.com)

Academic editor: *Franco Andreone* | Received 15 February 2011 | Accepted 5 May 2011 | Published 17 June 2011

urn:lsid:zoobank.org:pub:9B19F989-5202-4C66-87D8-FB1B568BA049

Citation: Páez-Moscoso DJ, Guayasamin JM, Yánez-Muñoz M (2011) A new species of Andean toad (Bufonidae, *Osornophryne*) discovered using molecular and morphological data, with a taxonomic key for the genus. ZooKeys 108: 73–97. doi: 10.3897/zookeys.108.1129

Abstract

Combining a molecular phylogeny and morphological data, we discovered a new species of *Osornophryne* from the Amazonian slope of the Ecuadorian Andes. Morphologically, the new taxon is distinguished from all others species in *Osornophryne* by having the Toes IV and V longer than Toes I–III, a short and rounded snout with a small rostral papilla, and conical pustules on flanks. The new species previously was confused with *O. guacamayo*. A taxonomic key is provided for all known species of *Osornophryne*.

Resumen

Al combinar una filogenia molecular con información morfológica, se descubrió una nueva especie de *Osornophryne* proveniente de la vertiente amazónica de los Andes del Ecuador. Morfológicamente, el nuevo taxón se distingue de los otras especies del género por tener los Dedos IV y V del pie más largos que los Dedos I-III, un rostro corto y redondeado con una pequeña papilla, y pústulas cónicas en los flancos

Copyright *Diego J. Páez-Moscoso et al.* This is an open access article distributed under the terms of the Creative Commons Attribution License, which permits unrestricted use, distribution, and reproduction in any medium, provided the original author and source are credited.

del cuerpo. La nueva especie estaba previamente confundida con *O. guacamayo*. Se provee de una clave taxonómica para todas las especies de *Osornophryne* reconocidas hasta la fecha.

Keywords
Andes, Bufonidae, Ecuador, new species, *Osornophryne,* phylogeny

Palabras Claves
Andes, Bufonidae, Ecuador, filogenia, especie nueva, *Osornophryne*

Introduction

Osornophryne is endemic to the Andes of Colombia and Ecuador, where it occurs in mountain forests and paramo at elevations between 2100 and 4000 m (Ruiz-Carranza and Hernández-Camacho 1976; Gluesenkamp and Guayasamin 2008; Muses-Cisneros et al. 2010). Currently, *Osornophryne* contains 10 recognized species: *O. angel* (Yánez-Muñoz et al. 2010), *O. antisana* (Hoogmoed 1987), *O. bufoniformis* (Peracca 1904), *O. guacamayo* (Hoogmoed 1987), *O. occidentalis* (Cisneros-Heredia and Gluesenkamp 2010), *O. percrassa* (Ruiz-Carranza and Hernández-Camacho 1976), *O. puruanta* (Gluesenkamp and Guayasamin 2008), *O. sumacoensis* (Gluesenkamp 1995), *O. talipes* (Cannatella 1986) and *O. cofanorum* (Muses-Cisneros et al. 2010). The evolutionary relationships between *Osornophryne* and other bufonid genera remain controversial, with some authors arguing a close affinity with *Atelopus* (Coloma 1997; Gluesenkamp 2001), and others supporting a topology in which *Osornophryne* is sister to most other bufonids (Bocxlaer et al. 2010). However, the monophyly of *Osornophryne* is well established by morphological and molecular characters (Ruiz-Carranza and Hernández-Camacho 1976; Coloma 1997; Gluesenkamp 2001; Bocxlaer et al. 2010); among the most conspicuous putative morphological synapomorphies are: six presacral vertebrae, digits almost completely embedded by an extensive membrane, reduced number or lenght of phalanges in hands and feet, absence of stapes and tympanum, urostlyle laterally expanded and broadly fused with sacrum, inguinal amplexus, and direct development (Ruiz-Carranza and Hernández-Camacho 1976; this work; compare with traits in South American bufonids; Pramuk 2006).

Given the complex topography of the Andes and the opportunity for allopatric speciation in areas with similar climatic conditions, it is possible that morphologically similar populations are evolving independently. Herein, we report and describe a new species of *Osornophryne,* previously confused with *O. guacamayo*.

Material and methods

Morphology. We examined alcohol-preserved specimens from the herpetological collections at Museo de Zoología of the Pontificia Universidad Católica del Ecuador (QCAZ),

Escuela Politécnica Nacional (EPN), and Museo Ecuatoriano de Ciencias Naturales (DH-MECN), all based in Quito, Ecuador. Specimens examined are listed in Appendix I. Fingers are numbered preaxially to postaxially from I–IV to facilitate comparison with previous literature dealing with anurans; however, we stress that in an evolutionary perspective anuran fingers should be numbered from II–V, consistent with the hypothesis that Digit I was lost in anurans (Shubin and Alberch 1986; Fabrezi and Alberch 1996). Morphological measurements were taken with digital calipers to the nearest 0.1 mm and are, as follow: (1) snout–vent length (SVL = distance from tip of snout [excluding the proboscis] to posterior margin of vent); (2) tibia length (TIB = length of flexed hind leg from knee to heel); (3) foot length (FL = distance from base of inner metatarsal tubercle to tip of Toe IV); (4) head length (HL = distance from tip of snout to articulation of jaw); (5) head width (HW = greatest width of head measured between jaw articulations); (6) interorbital distance (IOD = shortest distance between medial margins of upper eyelids); (7) upper eyelid width (EW = greatest width of eyelid measured perpendicular to medial axis of skull); (8) internarinal distance (IND = distance between internal borders of nostrils); (9) eye–nostril distance (EN = distance from anterior corner of eye to posterior border of nostril); (10) snout–eye distance (SE = distance from anterior corner of the eye to the tip of the rostrum); (11) eye diameter (ED = distance between anterior and posterior corners of eye); (12) Finger-III length (FIIIL = distance from proximal border of Finger I to distal end of Finger III); (13) Finger-IV length (distance from proximal border of Finger I to distal end of Finger IV); (14) Toe-IV length (TIVL = distance from proximal edge of Toe I to distal tip of Toe IV); (15) Toe-V length (TVL = distance from proximal border edge of Toe I to distal tip of Toe V). Sexual maturity was determinate by the presence of nuptial pads in adult males and convoluted oviducts in adult females. Techniques for clearing and double-staining specimens with Alcian Blue and Alizarin Red were those of Taylor and Van Dyke (1985). Illustrations were made with the aid of a Wild M3B Heerbrugg stereo dissecting microscope equipped with a camera lucida. Osteological terminology is that of Duellman and Trueb (1994), Fabrezi (1992, 1993), and Trueb (1973, 1993); bufonid osteological character states are illustrated in Pramuk (2006).

Molecular data. Fresh liver samples were preserved in 90% alcohol, and stored at –80°C. We used salt-precipitation protocols to extract genomic DNA from ethanol-preserved tissues (M. Fujita, unpubl. data). To amplify the mitochondrial gene 12S, we used the primers MVZ59 and tRNA-val, developed by Graybeal (1997) and Goebel et al. (1999), respectively; Polymerase Chain Reaction (PCR) amplification protocol was, as follows: 1 cycle of denaturation 2 min at 94°C, annealing for 30 sec at 42°C, extension for 1 min at 72°C, 5 cycles of denaturation 30 sec at 94°C, annealing for 30 sec at 42°C, extension for 1 min at 72°C, 22 cycles of denaturation 30 sec at 94°C, annealing for 30 sec at 50°C, extension for 1 min at 72°C, final extension at 72°C was conducted for 5 min. PCR products were visualized in 0.7% agarose gel, and unincorporated primers and dNTPs were removed from PCR products using ExoSap-it purification. Cycle sequencing reactions were conducted by the commercial company Macrogen Inc. Data from heavy and light stands were compared to generate a consensus sequence for each DNA fragment with Sequencer Ver. 4.8. We obtained sequences of 71 speci-

mens, including all the species in *Osornophryne,* except *O. talipes,* and three outgroup taxa. In addition, sequences were downloaded from GenBank (NCBI). Sequences were initially aligned in Clustal X (Larkin et al. 2007) and adjusted in Mesquite 2.71 (Maddison and Maddison 2009). Best-fit model of molecular evolution was selected in jModeltest 1.1 (Posada 2008) under the Akaike Information Criterion (AIC). Model parameters estimated from jModelTest were used in Bayesian analyses.

Phylogenetics. Analyses were conducted using Maximum Parsimony (MP), Maximum Likelihood (ML), and Bayesian Analyses (BA). Parsimony analyses were performed in PAUP (Swofford 2009) using heuristic searches (10,000 stepwise random additions with TBR branch-swapping) and clade support was estimated via 1000 bootstraps with 10 random additions. Maximum likelihood was run in GARLI 0.951 (Zwickl 2006), which uses a stochastic genetic algorithm-like approach to find the topology, branch lengths, and substitution model parameters that maximize the log-likelihood simultaneously (Zwickl 2006). We performed a total of 50 runs to reduce the probability of inferring a suboptimal likelihood solution. Node support was assessed via 1000 bootstrap replicates. For Bayesian analyses, we implemented the model of nucleotide substitution selected as the best fit for the particular dataset according to the Akaike Information Criterion (AIC) in jModeltest 1.1 (Posada 2008). Bayesian analysis of the mitochondrial dataset was performed in Mr Bayes 3.1 (Ronquist and Huelsenbeck 2003). The analysis consisted of 10 million generations and two Markov chains with default heating values. The prior used for the rate matrix was a uniform Dirichlet and no prior information on topology was incorporated. Trees were sampled every 1000 generations; stationarity was assessed by examining the standard deviation of split frequencies and by plotting the –lnL per generation using Tracer v1.4 (Rambaut and Drummond 2005), and trees generated before stationary were discarded as "burn-in." Bootstrap values $p > 70\%$ are considered to indicate strong support (Hillis and Bull 1993, with their caveats). Clades with posterior probabilities $p > 0.95$ are considered strongly supported, but we caution that relatively high posterior probabilities for short internodes (particularly those with low bootstrap values) may be overestimates of confidence (Alfaro et al. 2003; Erixon et al. 2003).

Results

For most of the species and population of *Osonophryne* and three species of *Atelopus*, we obtained a total of 800 bp from the mitochondrial marker 12S rRNA (Table 1). Parameter value estimates for best-fit models for 12S gene generated by jModeltest 1.1 are TIM2 + I (0.001) + G (0.4700). The only taxon for which we could not obtain molecular information was *O. talipes*, a species that, in Ecuador, is only know from a specimen collected on 02 August 1970 (Cannatella 1986). The different analyses (MP, ML, and AB) are congruent (Fig. 1). The topology resolves most of the relationships among species in *Osornophryne,* and reveals the presence of the previously unrecognized taxon described below.

Table 1. Summary of specimens sequenced of *Osornophryne* and *Atelopus* for the gen 12S and GenBank accession numbers.

Species and museum no.	Locality	Latitude and Longitude	GenBank No.
***Atelopus* sp.**			
QCAZ 34540	Limón		JF907488
QCAZ 41326	Zuruni		JF907486
QCAZ 38427	Las Tres Cruces		JF907487
Osornophryne angel			
QCAZ 40039	Páramo del Ángel	0°41'15"N, 77°52'46"W	JF907459
QCAZ 40036	Páramo del Ángel	0°41'15"N, 77°52'46"W	JF907458
QCAZ 40040	Páramo del Ángel	0°41'15"N, 77°52'46"W	JF907493
Osornophryne antisana			
QCAZ 40172	Páramo de Oyacachi	0°10'34"S, 78°0.6'50"W	JF907453
QCAZ 40173	Páramo de Oyacachi	0°10'34"S, 78°0.6'50"W	JF907485
QCAZ 40174	Páramo de Oyacachi	0°10'34"S, 78°0.6'50"W	JF907484
DH-MECN 838	Salvefaccha	0°13'54"S, 78°0.1'1"W	JF907490
DH-MECN 811	Salvefaccha	0°13'54"S, 78°0.1'1"W	JF907489
QCAZ 46204	Llanganates	1°15'57"S, 78°26'45"W	JF907450
QCAZ 46212	Llanganates	1°15'57"S, 78°26'45"W	JF907449
QCAZ 48035	Llanganates	1°15'57"S, 78°26'45"W	JF907448
QCAZ 48223	Llanganates	1°15'57"S, 78°26'45"W	JF907445
QCAZ 48220	Llanganates	1°15'57"S, 78°26'45"W	JF907446
QCAZ 48034	Llanganates	1°15'57"S, 78°26'45"W	JF907447
Osornophryne bufoniformis			
QCAZ 40123	Santa Bárbara	0°38'29"N, 77°31'18.5"W	JF907431
QCAZ 40121	Santa Bárbara	0°38'29"N, 77°31'18.5"W	JF907432
QCAZ 40003	Santa Bárbara	0°38'29.5"N, 77°31'18.5"W	JF907430
QCAZ 45082	Huaca	77°46'11"N, 0°40'15"W	JF907460
QCAZ 45083	Huaca	77°46'11"N, 0°40'15"W	JF907461
QCAZ 45084	Huaca	77°46'11"N, 0°40'15"W	JF907462
DH-MECN 1815	Playón de San Francisco	1°37'43"N, 77°54'35"W	JF907455
DH-MECN 1806	Playón de San Francisco	1°37'43"N, 77°54'35"W	JF907457
DH-MECN 1807	Playón de San Francisco	1°37'43"N, 77°54'35"W	JF907456
DH-MECN 1808	Playón de San Francisco	1°37'42.6"N, 77°54'35"W	JF907454
Osornophryne* cf. *bufoniformis			
QCAZ 9316	Vía Tulcán-Maldonado	0°47'31"N, 77°54'25"W	AF375498
Osornophryne cofanorum			
DH-MECN 1591	La Bonita	00°29'19"N, 77°35'11"W	JF907440
DH-MECN 1579	La Bonita	00°29'19"N, 77°35'11"W	JF907439
DH-MECN 1629	La Bonita	00°29'19"N, 77°35'11"W	JF907441
Osornophryne guacamayo			
QCAZ 40138	Poblado de Oyacachi	0°10'34"S,, 78°0'50"W	JF907463

Species and museum no.	Locality	Latitude and Longitude	GenBank No.
QCAZ 40143	Poblado de Oyacachi	0°10'34"S,, 78°0'50"W	JF907464
QCAZ 40147	Poblado de Oyacachi	0°10'34"S,, 78°0'50"W	JF907465
QCAZ 43370	Volcán Sumaco	0°34'11"S, 77°35'39"W	JF907474
QCAZ 4576	Volcán Sumaco	0°34'11"S, 77°35'39"W	JF907491
QCAZ 40106	Cordillera de los Guacamayos	0°37'26.5"S, 77°50'27"W	JF907468
QCAZ 40102	Cordillera de los Guacamayos	0°37'26.5"S, 77°50'27"W	JF907492
QCAZ 43554	Cordillera de los Guacamayos	0°37'26.5"S, 77°50'27"W	JF907467
QCAZ 17295	Volcán Reventador	77°40'44"S, 0°6'43"W	JF907471
QCAZ 17294	Volcán Reventador	77°40'44"S, 0°6'43"W	JF907473
QCAZ 17293	Volcán Reventador	77°40'44"S, 0°6'43"W	JF907472
QCAZ 12240	Río Angel	0°37'26.5"S, 77°50'27"W	JF907469
QCAZ 12241	Río Angel	0°37'26.5"S, 77°50'27"W	JF907470
QCAZ 2735	Jondachi (Río Angel)	0°37'26.5"S, 77°50'27"W	JF907466
QCAZ 46662	Santa Bárbara	0°33'51"N, 77°31'38"W	JF907475
Osornophryne occidentalis			
QCAZ 40028	Chilma	0°51'50"N, 78°4'1"W	JF907436
QCAZ 43652	Cuellaje	0°27'30"N, 78°32'43"W	JF907444
QCAZ 43498	Cuellaje	0°27'30"N, 78°32'43"W	JF907443
QCAZ 43653	Cuellaje	0°27'30"N, 78°32'43"W	JF907442
Osornophryne puruanta			
QCAZ 13271	Laguna de San Marcos	0°7'36"N, 78°15'22"W	JF907451
QCAZ 13320	Laguna de San Marcos	0°7'36"N, 78°15'22"W	JF907452
QCAZ 11471	Laguna de Puruanta	00°12' N, 77°57' W	AF375499.1
Osornophryne simpsoni			
QCAZ 49779	Llanganates	1°16'35"S, 78°4'21"W	JF907482
QCAZ 49777	Llanganates	1°16'35"S, 78°4'21"W	JF907477
QCAZ 49781	Llanganates	1°16'35"S, 78°4'21"W	JF907483
QCAZ 49776	Llanganates	1°16'35"S, 78°4'21"W	JF907476
QCAZ 39774	Río Zuñac	1°20'58"S, 78°09'31"W	JF907478
DH-MECN 5262	Río Zuñac	1°20'58"S, 78°09'31"W	JF907480
QCAZ 39778	Rio Zuñac	1°20'58"S, 78°09'31"W	JF907479
QCAZ 39773	Rio Zuñac	1°20'58"S, 78°09'31"W	JF907481
Osornophryne sumacoensis			
QCAZ 41243	Volcán Sumaco	0°34'11"S, 77°35'39"W	JF907434
QCAZ 41250	Volcán Sumaco	0°34'11"S, 77°35'39"W	JF907433
QCAZ 41246	Volcán Sumaco	0°34'11"S, 77°35'39"W	JF907437
QCAZ 41249	Volcán Sumaco	0°34'11"S, 77°35'39"W	JF907438
QCAZ 43379	Volcán Sumaco	0°34'11"S, 77°35'39"W	JF907435

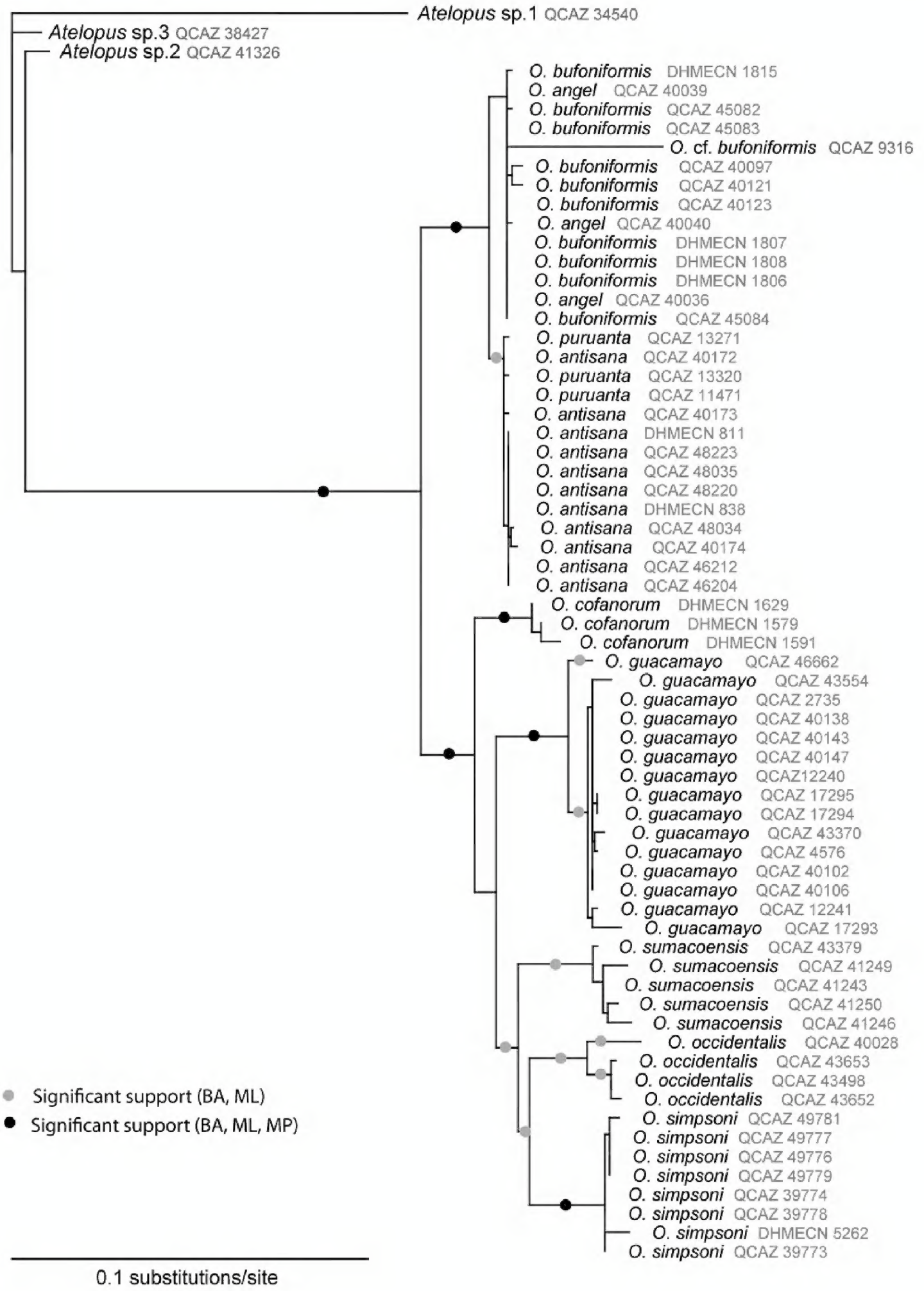
Atelopus sp.1 QCAZ 34540
Atelopus sp.3 QCAZ 38427
Atelopus sp.2 QCAZ 41326
O. bufoniformis DHMECN 1815
O. angel QCAZ 40039
O. bufoniformis QCAZ 45082
O. bufoniformis QCAZ 45083
O. cf. bufoniformis QCAZ 9316
O. bufoniformis QCAZ 40097
O. bufoniformis QCAZ 40121
O. bufoniformis QCAZ 40123
O. angel QCAZ 40040
O. bufoniformis DHMECN 1807
O. bufoniformis DHMECN 1808
O. bufoniformis DHMECN 1806
O. angel QCAZ 40036
O. bufoniformis QCAZ 45084
O. puruanta QCAZ 13271
O. antisana QCAZ 40172
O. puruanta QCAZ 13320
O. puruanta QCAZ 11471
O. antisana QCAZ 40173
O. antisana DHMECN 811
O. antisana QCAZ 48223
O. antisana QCAZ 48035
O. antisana QCAZ 48220
O. antisana DHMECN 838
O. antisana QCAZ 48034
O. antisana QCAZ 40174
O. antisana QCAZ 46212
O. antisana QCAZ 46204
O. cofanorum DHMECN 1629
O. cofanorum DHMECN 1579
O. cofanorum DHMECN 1591
O. guacamayo QCAZ 46662
O. guacamayo QCAZ 43554
O. guacamayo QCAZ 2735
O. guacamayo QCAZ 40138
O. guacamayo QCAZ 40143
O. guacamayo QCAZ 40147
O. guacamayo QCAZ12240
O. guacamayo QCAZ 17295
O. guacamayo QCAZ 17294
O. guacamayo QCAZ 43370
O. guacamayo QCAZ 4576
O. guacamayo QCAZ 40102
O. guacamayo QCAZ 40106
O. guacamayo QCAZ 12241
O. guacamayo QCAZ 17293
O. sumacoensis QCAZ 43379
O. sumacoensis QCAZ 41249
O. sumacoensis QCAZ 41243
O. sumacoensis QCAZ 41250
O. sumacoensis QCAZ 41246
O. occidentalis QCAZ 40028
O. occidentalis QCAZ 43653
O. occidentalis QCAZ 43498
O. occidentalis QCAZ 43652
O. simpsoni QCAZ 49781
O. simpsoni QCAZ 49777
O. simpsoni QCAZ 49776
O. simpsoni QCAZ 49779
O. simpsoni QCAZ 39774
O. simpsoni QCAZ 39778
O. simpsoni DHMECN 5262
O. simpsoni QCAZ 39773
Significant support (BA, ML)
Significant support (BA, ML, MP)
0.1 substitutions/site

Figure 1. Maximum likelihood phylogeny of the species in *Osornophryne* inferred from the mitochondrial gene 12S (lnL = –1384,3649).

***Osornophryne simpsoni* sp. n.**
urn:lsid:zoobank.org:act:9BFBC919-F698-4FDE-8994-9154FF9E99ED
http://species-id.net/wiki/Osornophryne_simpsoni

Holotype. QCAZ 49774 (Figs 2, 3), an adult male near San Rafael-Chontayacu (1°16'34.61"S, 78°4'21.14"W, 2266 m.a.s.l.), Reserve Ankaku-Zona, Río Challuwayacu, Provincia de Pastaza, Ecuador, by Elicio Tapia on 21 October 2009.

Paratopotypes: QCAZ 48781, 49777, 45899 obtained with holotype.

Paratypes. DH-MECN 5660 adult female, DH-MECN 5261, 5263, 5258–59, adult male obtained near Reserva Biológica Río Zuñac (1°20'57,87"S, 78°09'31,37"W, 2250 m.a.s.l.), Parroquia Río Negro, Cantón Baños, Provincia de Tungurahua, Ecuador, by MYM, M. Urgiles y A. Laguna on 17 May 2008; QCAZ 39769 also obtained near Reserva Biológica Río Zuñac, by DJP, A. Narváez, and J. P. Reyes-Puig on 21 January 2009.

Diagnosis. *Osornophryne simpsoni* differs from all other species in *Osornophryne* (except for *O. guacamayo* and *O. cofanorum*) by having Toes IV and V longer than Toes I–III (Fig. 4). Morphologically, *O. simpsoni* is most similar to *O. guacamayo;* both species have Toes IV and V longer than Toes I–III, pustular dorsal skin, and dark brown dorsal coloration. However, *O. simpsoni* lacks the conspicuos proboscis present in *O. guacamayo;* males of *O. simpsoni* can be distinguished from males of *O. guacamayo* by having ventral skin with conical pustules (non-conic pustules in *O. guacamayo*), and light brown to orange conical pustules on the flanks (dark brown to black non-conical pustules in *O. guacamayo*); the venter of female *O. guacamayo* is mostly whitish to yellowish with brown marks, whereas that of female *O. simpsoni* is orange-brown. *Osornophryne cofanorum* differs from *O. simpsoni* by having its vertebrae and urostlyle coosified with the overlying skin (not co-osified in *O. simpsoni*) and vertebral neural spines that are visible dorsally (not visible in *O. simpsoni*); also, males of *O. cofanorum* have yellow pustules on the tip of the snout, upper eyelid, limbs, and dorsolateral pustular clusters (absent in *O. simpsoni*). Finally, *O. simpsoni* is distinguished from its sister species, *O. occidentalis,* by having a rounded snout in lateral view (protruding in *O. occidentalis*), brown dorsum with some lighter patches (dark brown dorsum with dark ochre-brown warts in *O. occidentalis*), orange-brown venter (white in *O. occidetalis*), and by inhabiting in the Amazonian slopes of the Andes (*O. occidentalis* is found on the Pacific slopes of the Andes).

Species Description. Ten adult males and one adult female. Females of medium size (SVL = 33.0 mm, n = 1); males small (SVL = 17.6–26.1 mm; mean = 21.1 ± 2.40, n = 10; Table 2). Head length 77.2–95.1% head width; male head width 34.9–40.8% SVL; female head width 37.3% SVL; width of head greater at level of posterior margin of mouth; snout short, rounded, with rostral papilla in dorsal and lateral views; nostrils slightly swollen; each nostril oblique, oval, directed laterally; internarial area concave in males and slightly concave in female; interorbital region with skin co-osified with underlying bone, which has few low tubercles; occipital region mostly flat, but with few bony tubercles and cranial crests in males and females; upper eyelids finely tuber-

Figure 2. *Osornophryne simpsoni* sp. n. in life (male holotype, QCAZ 49774).

culate in females, with conical tubercles in males; interorbital region wider than the upper eyelid (upper eyelid 73.0–87.5% of interorbital distance in males, $n = 9$; 64.4% in female); outer edge of the eyelid delineated by a continuous row of warts, which are more conical in males than in female; canthus rostralis straight; loreal region slightly concave, with small warts in males and female; pale brown lips; eyes with oval horizontally pupil; infraorbital and postorbital regions with some prominent tubercles of variable size in males and females. Skin of dorsum highly tuberculate, with discontinuous row of conical tubercles starting at level of posterolateral edge of cranium and ending at level of sacrum in males and females; in males, ventral skin with several small pustules and few conical tubercles on gular region and toward the flanks, pustules much denser on chest and abdomen and less conical; in females, ventral skin smooth, with small, non-conical isolated pustules, pustules more numerous on abdomen.

Forelimb long, slender, finely granular, with several larger tubercles extending along inner and outer edges of fingers in males; in females, tubercles smaller than in males. Hand of moderate length, representing 25.0–30.4% ($n = 10$) of SVL in males and 28.5% in female; extensive webbing between fingers (Fig. 4); lengths of fingers in order of increasing length : I < II < IV < III; palms with numerous tubercles; subarticular tubercles not distinguishable; palmar tubercle rounded, thenar tubercle almost undistinguishable.

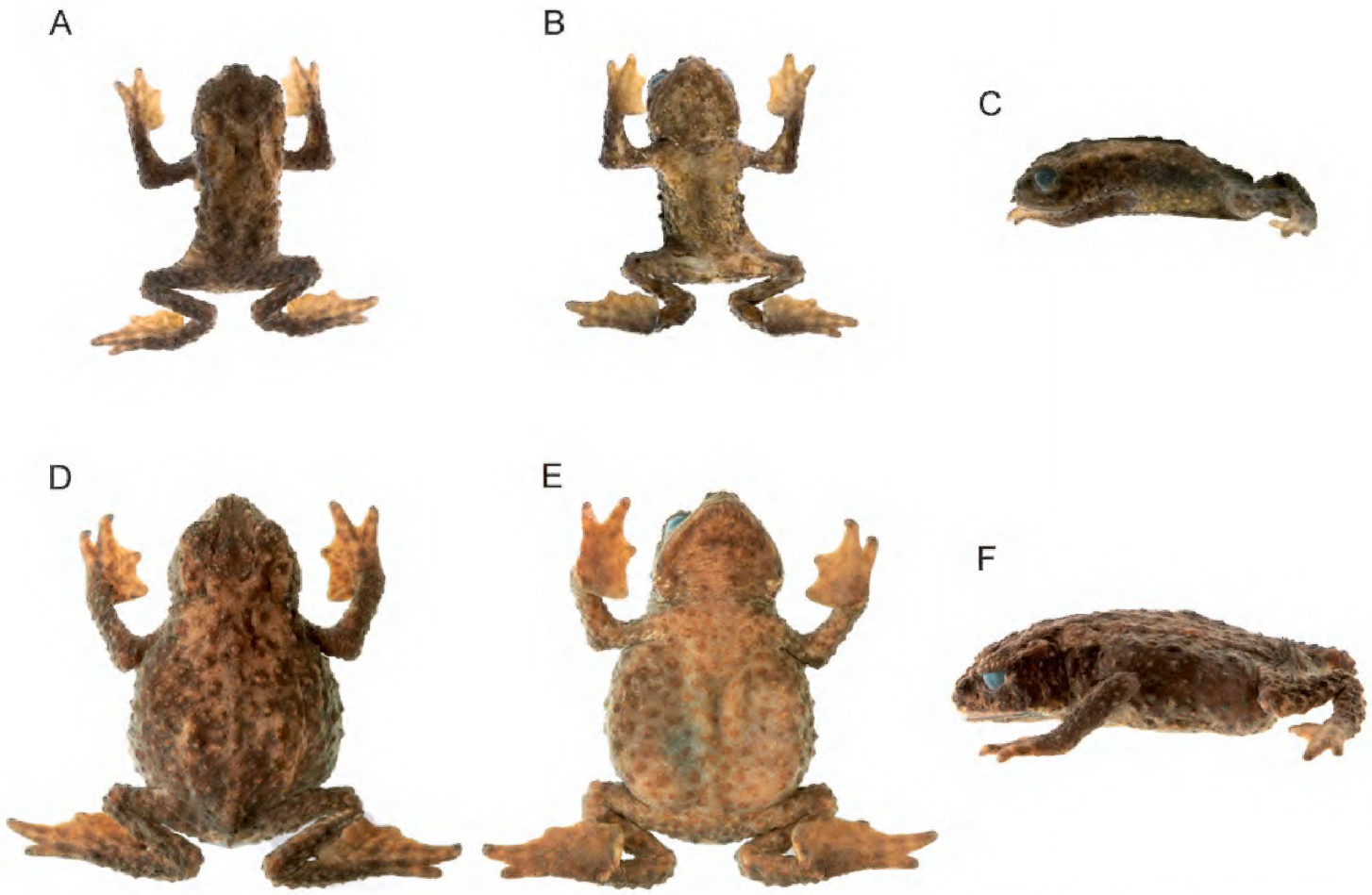

Figure 3. *Osornophryne simpsoni* sp. n. in alcohol. **A–C** Dorsal, ventral and lateral views of holotype, adult male, QCAZ 49774, SVL 20.1 mm **D–F** Dorsal, ventral and lateral views of adult female, DH-MECN 5260, SVL 33.0 mm.

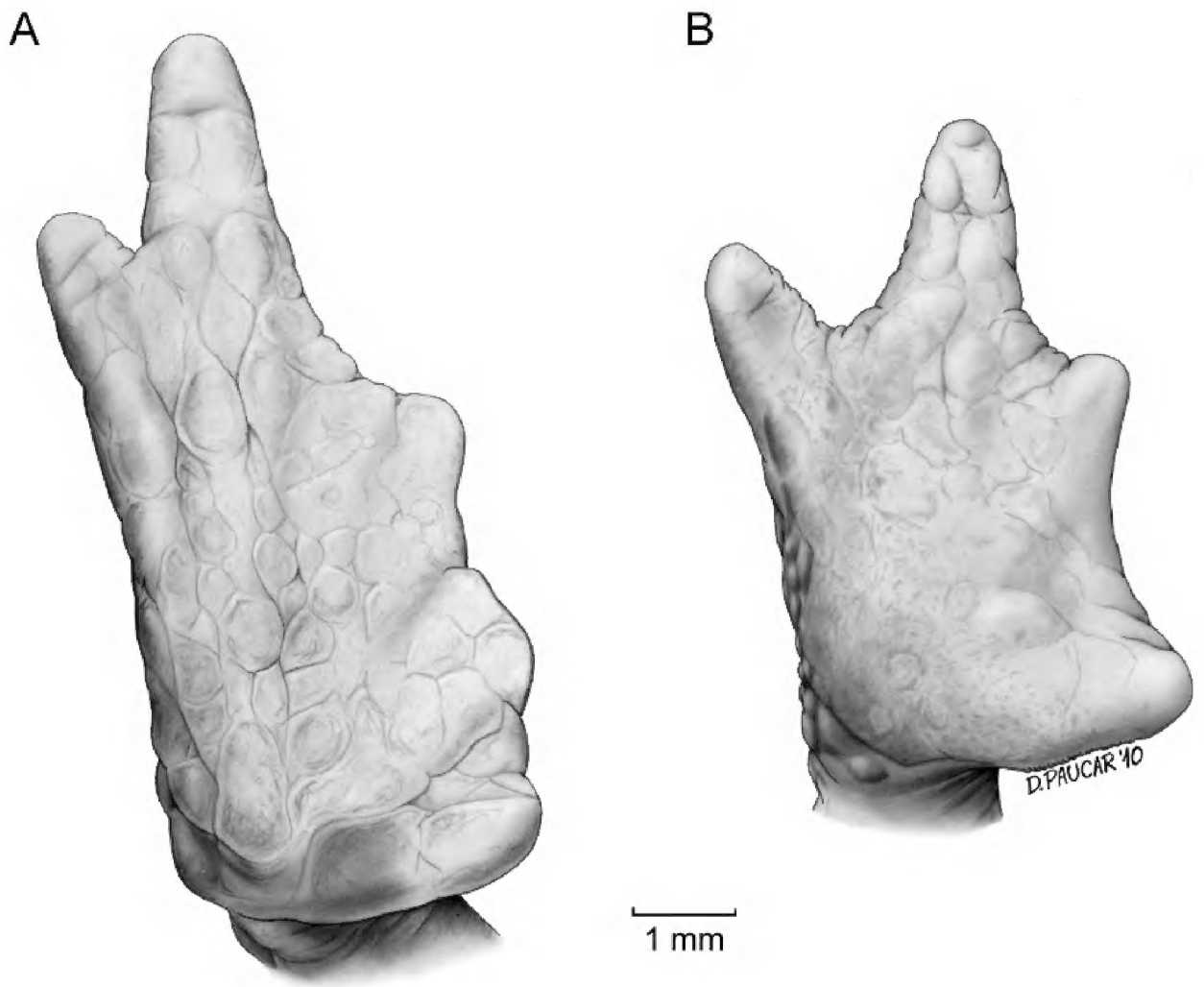

Figure 4. Foot (**A**) and hand (**B**) of *Osornophryne simpsoni* sp. n. (holotype, adult male, QCAZ 49774).

Table 2. Morphometrics of adult males and female of *Osonophryne simpsoni* sp. n.

Museum number	Sex	SVL	HL	HW	FL	TIB	IOD	EW	IND	IND	FIIIL	FIVL	LM	LF	TL	EN	ED
DH-MECN 5260	Female	33.0	9.5	12.3	13.8	11.4	5.9	3.8	3.1	3.1	8.4	9.4	8.3	13.0	11.2	2.8	3.2
QCAZ 49774	Male	20.1	7.2	8.2	8.4	6.8	3.4	2.8	2.3	2.3	5.3	5.7	5.4	8.0	7.2	1.7	2.9
QCAZ 45899	Male	19.5	6.4	7.6	7.0	5.7	3.7	2.7	1.9	1.9	4.5	5.2	4.9	6.6	6.5	1.7	2.8
QCAZ 49777	Male	17.6	5.9	6.7	7.0	5.6	3.2	2.8	2.0	2.0	4.2	4.6	4.4	6.3	5.9	1.5	2.8
QCAZ 49781	Male	18.6	6.0	7.0	7.1	5.6	3.1	2.6	2.1	2.1	4.6	5.0	4.5	6.5	6.1	1.6	2.1
QCAZ 39774	Male	23.2	7.7	8.1	8.5	7.4	4.0	1.8	2.1	2.1	5.3	5.8	5.3	7.6	7.9	1.9	2.6
QCAZ 39769	Male	26.1	8.2	9.4	9.1	7.7	4.0	3.0	3.0	3.0	6.3	6.6	5.8	8.9	8.8	2.0	2.7
DH-MECN 5261	Male	21.5	7.2	8.0	8.7	7.4	4.1	3.2	2.2	2.2	5.7	6.2	5.4	7.6	7.1	1.9	4.1
DH-MECN 5259	Male	21.4	6.8	8.1	9.1	7.7	4.0	3.1	2.6	2.6	5.8	6.5	5.8	9.3	7.9	2.0	4.0
DH-MECN 5258	Male	21.2	7.2	8.4	8.1	6.8	3.8	2.8	2.6	2.6	5.3	5.8	5.4	8.8	7.6	2.1	3.8
DH-MECN 5263	Male	21.3	6.8	8.0	8.8	7.5	3.6	3.0	2.7	2.7	5.5	5.8	5.3	7.9	7.5	1.8	3.6

Hind limbs long and slender; well-defined pustules present on inner and outer edges of fingers in males, females with less pronounced pustules than those in males; tibia and foot, respectively, 32.8–36.9% and 34.9–42.5% of male SVL, and 33.9% and 41.9% of female SVL; webbing between Toes I–III more extensive that webbing between Toes IV–V (Fig. 4); lengths of Toes: I < II < III < V < IV; Toe V much longer than Toe III, soles with numerous tubercles; subarticular tubercles indistinguishable; inner metatarsal tubercle oval. Choanae slightly rounded; adult males lacking vocal sacs; vocal slits absent; nuptial pads on proximal surfaces of Toes I and II, not pigmented; cloacal opening medial to thighs.

Coloration in alcohol. Dorsum, head, forearms, and hind limbs brown to dark brown, with some orange patches; tubercles on upper eyelid, proboscis, and flanks pale yellow. Throat pale yellow; venter cream with brown tubercles.

Coloration in life. Dorsum, head, forearms, and hind limbs dark brown to light brown with some lighter patches; tubercles on upper eyelid, proboscis and flanks orange to yellow. Throat cream yellow, with small dark marks; venter orange-brown.

Osteology. The following osteological description of *Osornophryne simpsoni* is based on a cleared-and-double stained adult male (QCAZ 45899, SVL = 19.5 mm). The osteological description of females was not possible because only one female is known.

Cranium. *Shape and proportions.* The skull is widest posterior to the orbit at the level of the articulation of the maxilla with the quadratojugal. The braincase is broad; at the level of the midorbit, the width of the braincase is about 41.2% of the greatest width of the skull and 26.2% of the medial skull length.

Neurocranium. The neurocranium is formed by five bones—the sphenethmoid, and the paired prootics and exoccipitals. Anteriorly, the neurocranium is completely ossified. A minute septomaxilla is embedded in the anterior nasal capsule cartilage. In dorsal aspect, the cartilaginous planum antorbitale has a perpendicular orientation in relation to the longitudinal axis of the skull. In lateral and ventral views, a broad cartilaginous separation between bony sphenethmoid and prootic is evident. The frontoparietal fontanelle is partially exposed medially between the frontoparietals. Distally, the otic capsules are cartilaginous. Medially, the exoccipitals are slightly separated from one another. The dorsal surface of each prootic is smooth. The epiotic eminences are prominent.

Auditory apparatus. The stapes and tympanic annulus are absent. The operculum is oval and cartilaginous.

Dermal investing bones. Dorsal investing bones are well developed. The nasals are separated from one another and cover most of the nasal capsules dorsally. The maxillary process of the nasal overlaps the pars fascialis of the maxilla to form a bony anterior margin of the orbit. The frontoparietals are well developed and have a narrow separation between one another along its longitudinal axis. The posteriormedial margin of each frontoparietal contacts the exoccipital, but is not fused to it. Posterolateraly, each frontoparietal bears a bony extension that reaches the epiotic eminence. Each frontoparietal has a lamina perpendicularis that is narrow anteriorly and greatly expanded posteriorly

(Fig. 5C). The dorsal surface of each frontoparietal bears small, bony tubercles that are visible externally; the tubercles seem to be co-ossified with the overlying skin.

Ventral investing and palatal bones. The parasphenoid has the shape of an inverted T. The broad cultriform process extends anteriorly to about the mid-level of the orbit, where it is narrowly separated from the posterior border of the sphenethmoid. The cultriform process reaches its maximum width at a level that is coincident with the posterior margin of the optic fenestra. The parasphenoid alae are robust, investing the cartilaginous floor of the otic capsule anterior to the exoccipitals; the length of each ala is 61.8% the length of the cultriform process. A broadly acuminate posteromedial process of the parasphenoid terminates just anterior to the margin of the foramen magnum. The vomers are small, arcuate, broadly separated bones that support the medial margins of the choanae; the bones are unornamented, edentate, and lack dentigerous processe; the prechoanal ramus of the vomer is especially short. The neopalatine is short and narrow; medially, it reaches the anterolateral margin of the sphenethmoid; medially, the neopalatine does not contact the maxilla (Fig. 5B).

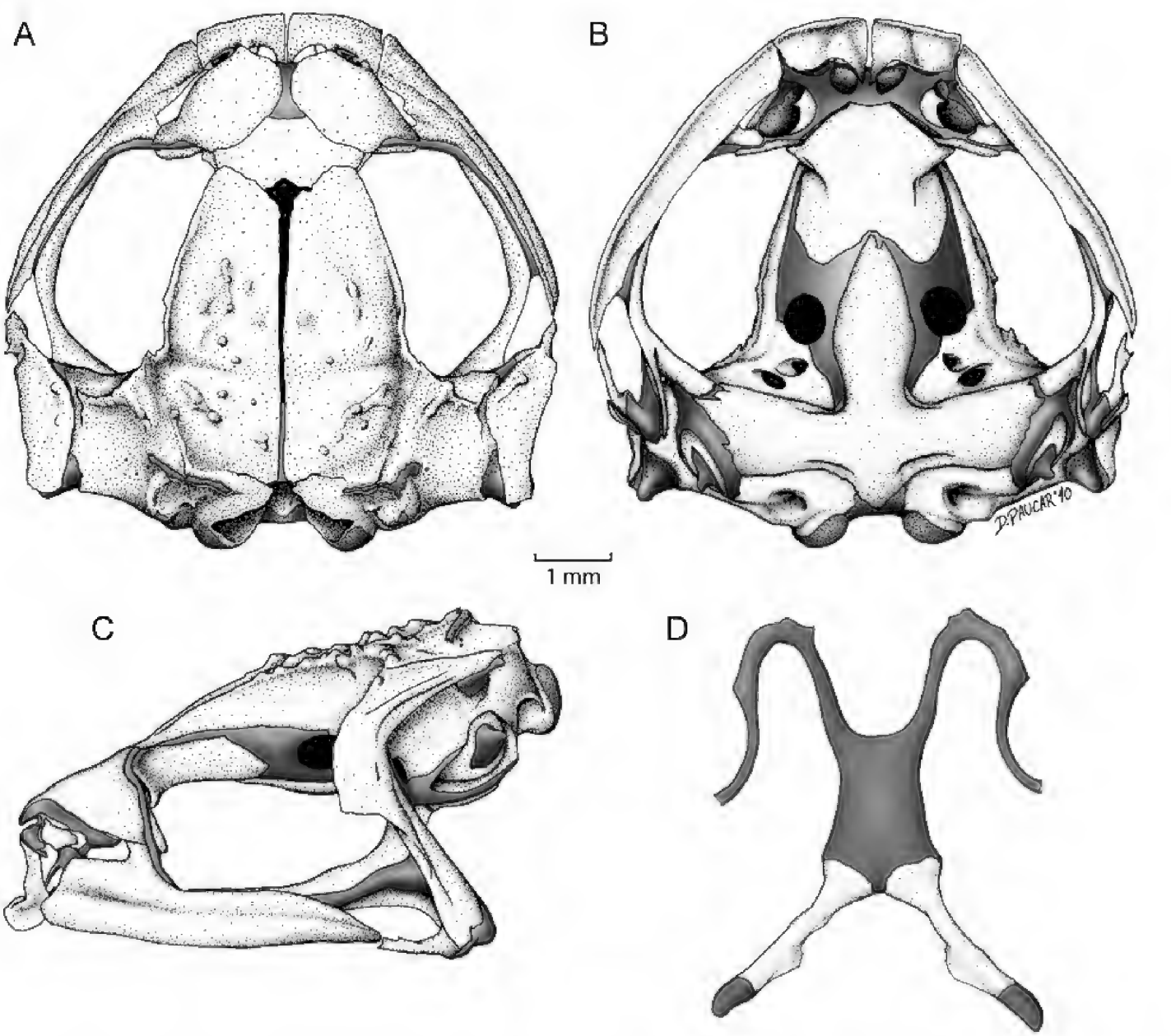

Figure 5. Skull and hyoid of *Osornophryne simpsoni* sp. n., adult male, QCAZ 45899. **A** Dorsal view of skull **B** Ventral view of skull **C** Lateral view of skull **D** Ventral view of hyoid.

Maxillary arcade. The premaxillae and maxillae lack teeth. The arcade is complete and has a tenuous articulation with the short quadratojugals. The pars palatinae of the premaxillae are broad. The premaxilla bears two palatine processes, a narrow longer medial and a broad lateral process. There is a simple, juxtaposed articulation between the anterior end of the maxilla and the premaxilla. The pars facialis of the maxilla is well-developed anteriorly, covering the the posterior region of the olfactory capsule; also, the pars facialis has a well-developed preorbital process, which covers most of the planum antorbitale (Fig. 5B, C).

Suspensory apparatus. The tridiate pterygoid bears a slightly curved anterior ramus that is orientated anterolaterally toward the maxilla, with which it articulates. The pterygoid is in close proximity to the maxilla and the narrow space between them is filled by the pterygoid cartilage. The medial and posterior rami of the pterygoid are about equal in length; however, the medial ramus is more robust than the posterior. The lateral end of the medial ramus overlaps the lateral edge of the prootic. The squamosal has the shape of an inverted L; the zygomatic ramus is almost absent, whereas the otic ramus is long and almost reaches the posterior end of the skull. The otic ramus overlaps the lateral margin of the crista parotica slightly. The ventral ramus invests the lateral surface of the palatoquadrate, and articulates with the quadratojugal (Fig. 5A, C); along its anterior margin, the ventral ramus has a conspicuos flange, which extends along the upper border of the otic ramus (Fig. 5C).

Hyoid. The width of the cartilaginous hyoid corpus is narrower than its medial length (width 63.1% of length). The anterolateral and posterolateral processes of the hyoid are absent. The bony posteromedial processes are slightly expanded proximally; each process has a bony flange along the posteromedial margin. The hypoglossal sinus is broadly U-shaped. The hyalia are simple and lack any processes (Fig. 5D).

Postcranium. *Vertebral column*. There are six prepresacral vertebrae. Presacrals I and II are not fused and are notably shorter than Presacrals III–VI. The vertebral profile in decreasing order of overall width of bony parts is: Sacrum > III > IV > V > VI > II > I. Presacral I, or the atlas, lacks transverse processes. All presacrals are non-imbricate. The transverse processes of Presacral II have a anterolateral orientation, Presacrals III–V have a slightly posterolateral orientation, and Presacral VI is approximately perpendicular to the longitudinal axis of the body. The bony sacral diapophyses are broadly expanded; posteriorly, the sacrum is broadly fused with the urostyle, which is greatly expanded laterally. The urostyle bears a well-developed dorsal crest throughout most of its length (Fig. 6).

Pectoral girdle. The clavicles have a slight orientation, with the medial tips distinctly separated from one another and located at about the same level of the anterolateral end of the clavicle, which articulates with the pars acromialis of the scapula (Fig. 7). The coracoid is notably stout, with the sternal end having a moderate expansion and the sternal end being heavily expanded (sternal end 45% of glenoid end); the inner edge of coracoid has an angle of about 45°, wheras the external edge is straight (no angle). The pectoral fenestra is has a tringular shape, in which the base is anteriorly convex. The scapula is moderately long with a prominent pars acromialis

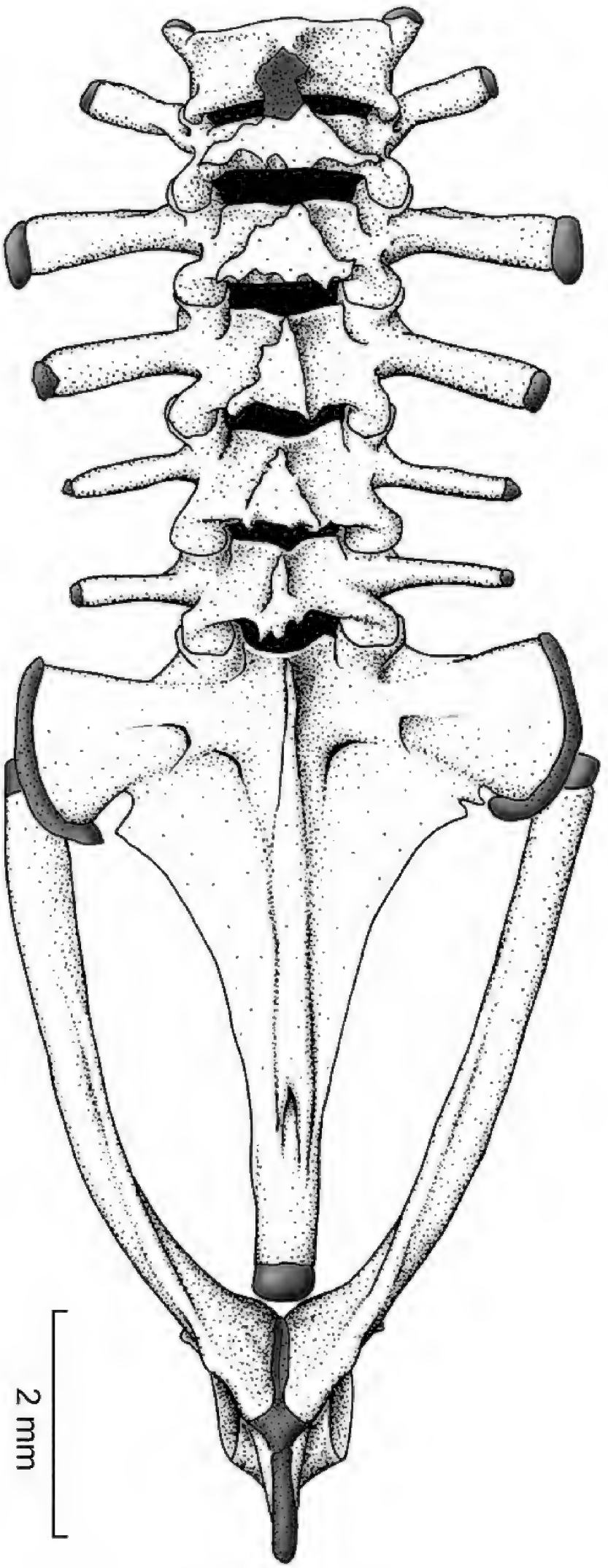

Figure 6. Vertebral column of *Osornophryne simpsoni* sp. n. in dorsal view; adult male, QCAZ 45899.

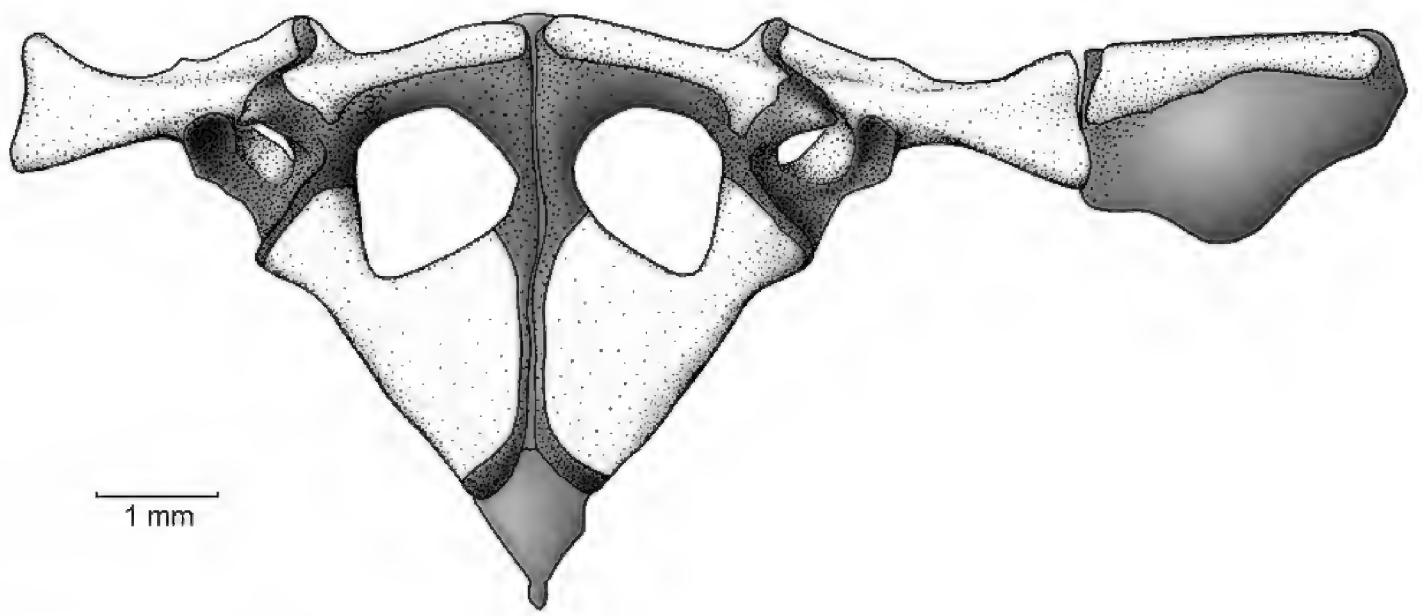

Figure 7. Pectoral girdle of *Osornophryne simpsoni* sp. n. in ventral view; adult male, QCAZ 45899.

that is separated from the pars glenoidalis; the leading and posterior edges of the scapula are slightly concave. The suprascapula is mostly cartilaginous, but it is mineralized at both ends, with the ossified cleithrum apparent as a slender bone along the leading edge of the suprascapular blade and with a proximal end that is wider than its distal end. The sternum is small and completely cartilaginous; it contacts the epicoracoid cartilage, which is extensive, and the posterior margin of the coracoid. The omosternum is absent.

Pelvic girdle. The long, slightly concave, and slender ilial shafts bear small dorsal crests, which extend from the anterior third to the posterior end of the shafts (Fig. 6). The ilial prominence is broad and low; the pubes is highly mineralized.

Manus and pes. The phalangeal formulae for the hand and foot are standard—i.e., 2-2-3-3 and 2-2-3-4-3, respectively; however, the distal phalange of Finger I, Toe I, and Toe III are greatly reduced and formed mostly by cartilage (Fig. 8). Relative length of fingers, in increasing order, is: I-II-IV-III, and of the foot is: I-II-III-V-IV. The carpus is composed of a radiale, ulnare, Element Y, Carpal 2, and a large postaxial assumed to represent a fusion of Carpals 3–5. Element Y is about 3 times the size of Carpal 2, and the prepollex is an elongated cartilage. The terminal phalanges are acuminate, except Finger III that is slightly T-shaped. The tarsus is composed of two tarsal elements, presumably Tarsal 1 and Tarsal 2 + 3. The prehallux is presented by a proximal mineralized cartilage element associated with a small bony element.

Etymology. The specific name *simpsoni* is a patronym for Dr. Nigel Simpson in recognition for his continual efforts in protecting the Andean cloud forests of Ecuador. Dr. Simpson is a collaborator of two of the most important conservation NGOs in Ecuador, EcoMinga Foundation (www.ecominga.net) and Jocotoco Foundation (www.fjocotoco.org). As the common name of the species, we suggest "Simpson's Plumb Toad." In Spanish, we suggest the name "Osornosapo de Simpson."

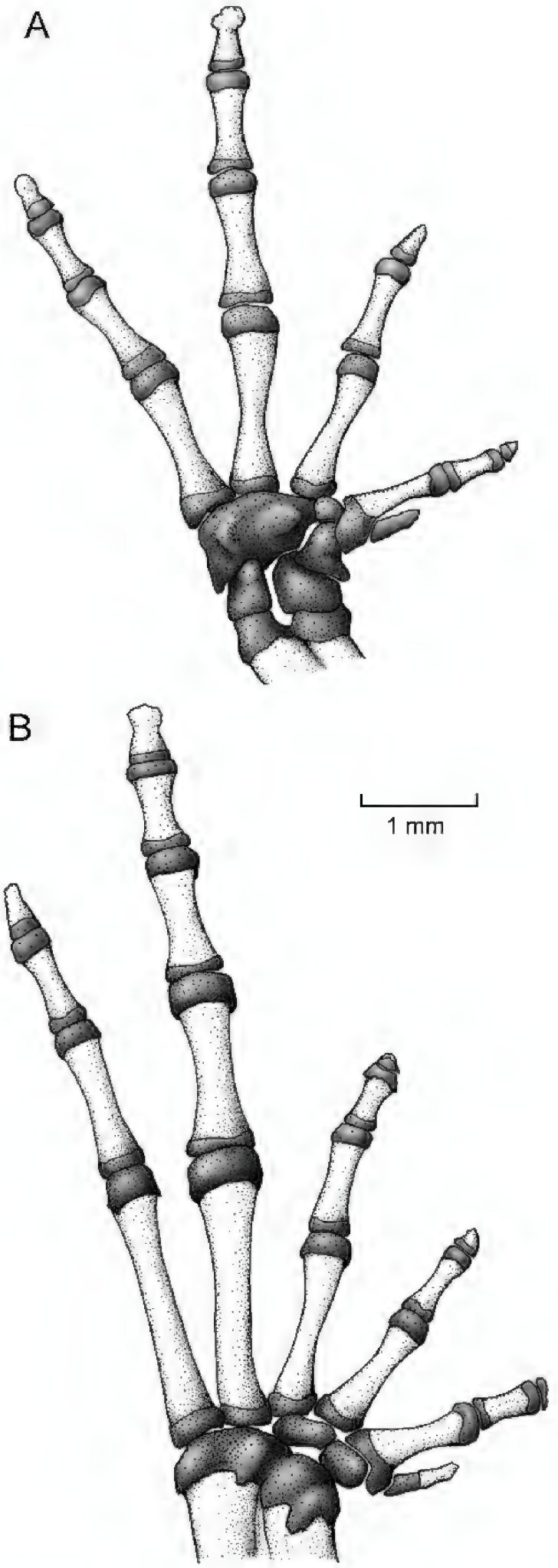

Figure 8. Osteology of hand and foot of *Osornophryne simpsoni* sp. n. in ventral view; adult male, QCAZ 45899.

Distribution and conservation. *Osornoprhyne simpsoni* is only known from the type locality and surrounding areas, Reserva Zuñac (1°20'58"S, 78°09'31"W) and Reserve Ankaku-Zona (1°16'35"S, 78°4'21"W; Fig. 9). These localities are included in the Bosque de Niebla Montano (Montane Cloud Forest) according to the classification proposed by Valencia *et al.* (1999). Vegetation is dominated by Clusia spp. trees. All individuals of *O. simpsoni* have been found on leaves of bromeliads and ferns during the night. Simpatric anurans include *Pristimantis altamis, P. bicantus, P. imcomptus* and *P. galdi*. Following the IUCN (2001) criteria, we consider *O. simpsoni* as Data Deficient; however, it is likely that *O. simpsoni* has a restricted distribution, as observed in other *Osornophryne* species.

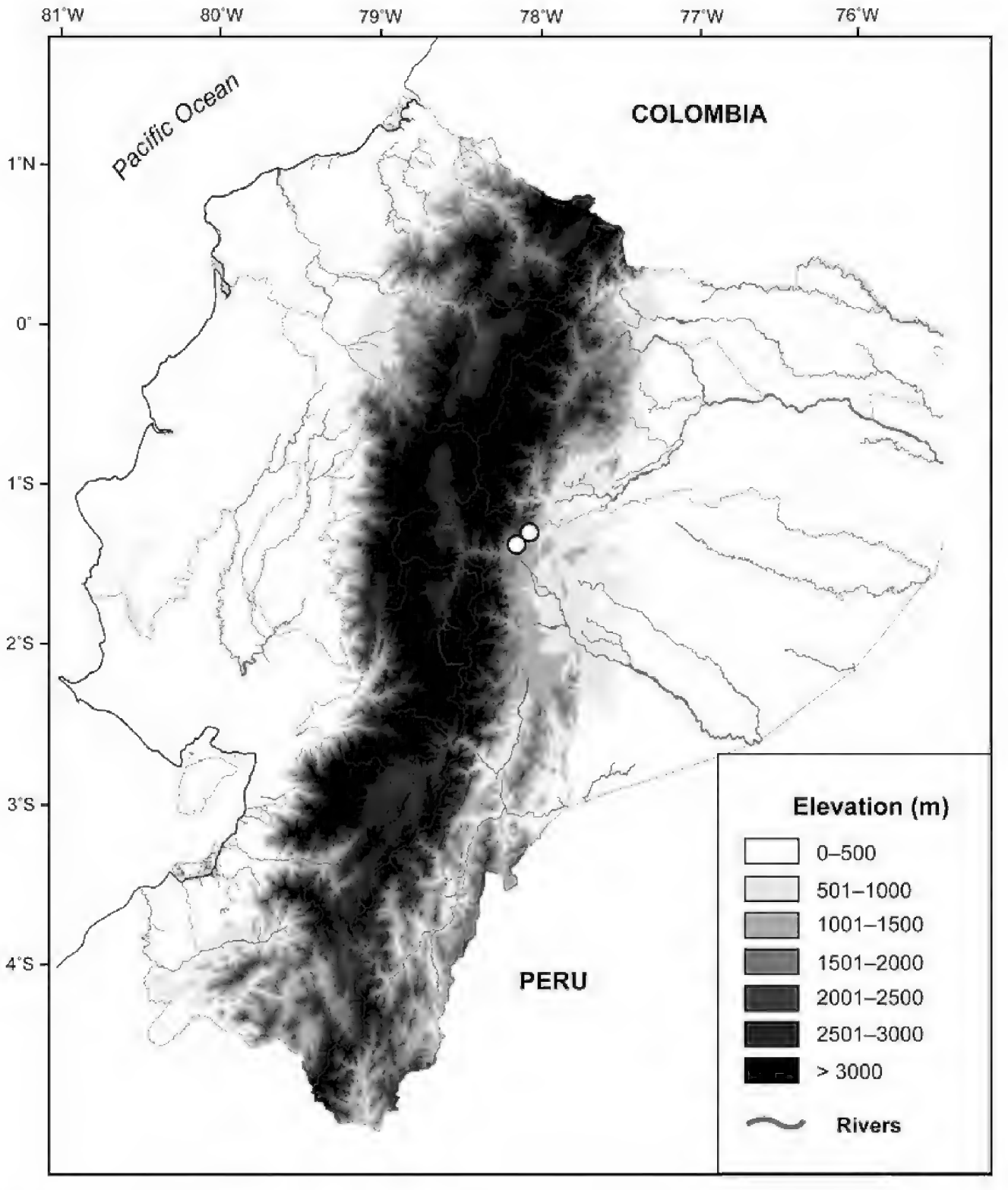

Figure 9. Distribution of *Osornophryne simpsoni* sp. n. (white circles) in Ecuador.

Discussion. It has become increasingly evident that lineage independence is not always accompanied by morphological change when ecological conditions remain similar (Wiens 2004). Therefore, combining different sources of data in the process of species discovery increases the probabilities of revealing evolutionary species (sensu Simpson 1961; Wiley 1978; Padial et al. 2009). The discovery of *Osornophryne simpsoni* represents a good example of such approach. The phylogeny presented in Figure 1 shows some interesting issues that will need further research. For example, given the current gene sampling, there is no genetic differentiation between *O. angel* and *O. bufoniformis;* similarly, *O. antisana* and *O. puruanta* are not reciprocally monophyletic, although they have conspicuous morphological differences (e.g., body size). Last, within *O. guacamayo*, there are two genetically distinctive populations that might represent evolutionary species.

Key to the species of *Osornophryne*

1 Toe V longer than Toes I–III (Fig. 4A) **2**
– Toe V shorter than Toes I–III **4**
2 Vertebrae and urostyle co-ossified with overlying skin; in life, males with yellow pustules on upper eyelid and tip of snout ..... ***O. cofanorum***
– Vertebrae and urostyle not coossified with overlying skin; males lacking yellow pustules on tip of snout **3**
3 Head acuminate, with a long proboscis (Figs 10, 11); dorsal skin lacking conical tubercles in most populations (except population from Volcán Sumaco); dorsum dark brown to black, sometimes with grayish-yellow dorsolateral stripes ..... ***O. guacamayo***
– Head with short and round snout, with small papillae at tip (Figs 10, 11); dorsal skin with conical tubercles; dorsum lacking dorsolateral stripes (Fig. 2) ..... ***O. simpsoni***
4 Dorsum covered with numerous round pustules of different sizes (lacking space among pustules) **5**
– Dorsum with sparsely distributed pustules (space among pustules clearly evident) **6**
5 Female dorsal skin highly tuberculate, with prominent dorsolateral ridges; flanks with large rounded pustules; males and females with prominent occipital ridges; in males, head acuminated to subacuminated in lateral view (Figs 10, 11) ..... ***O. angel***
– Female dorsal skin highly tuberculate, with faintly defined dorsolateral ridges; flanks with scattered and small pustules; males and females with low (or lacking) occipital ridges; in males, head rounded or truncated in lateral view (Figs 10, 11) ..... ***O. bufoniformis***
6 Dorsolateral, occipital, and pelvic ridges separated by smooth skin 7
– Dorsolateral, occipital, and pelvic ridges separated by flat pustules **9**

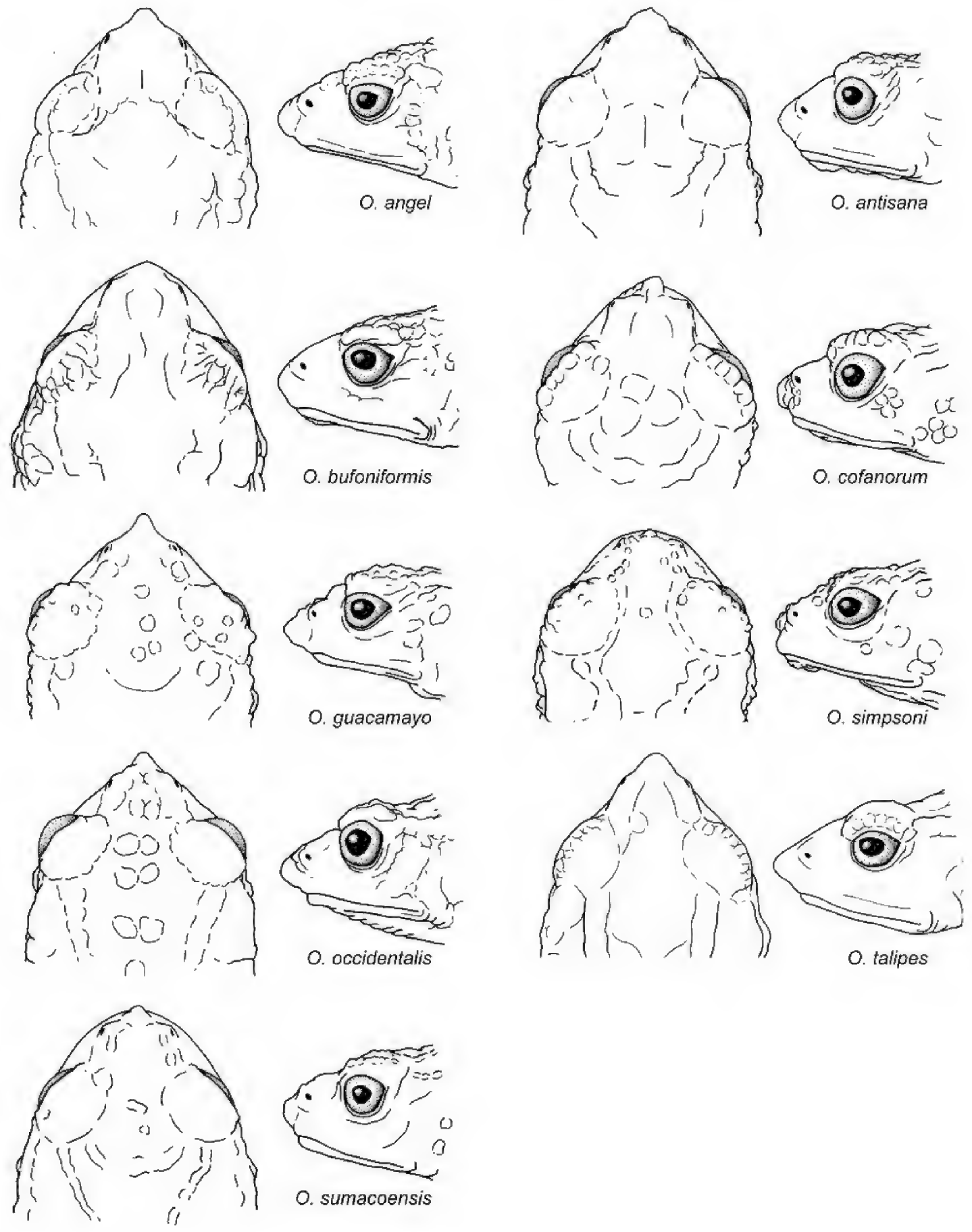

Figure 10. Head shape in dorsal and lateral views of *Osornophryne* males. Illustrated species are: *O. angel,* QCAZ 40048; *O. antisana,* QCAZ 48209; *O. bufoniformis,* QCAZ 45084; *O. cofanorum,* DH-MECN 6248; *O. guacamayo,* QCAZ 40106; *O. simpsoni,* QCAZ 49774; *O. occidentalis,* QCAZ 43529; *O. sumacoensis,* QCAZ 41246; *O. talipes,* ICN 12256. Not drawn at scale.

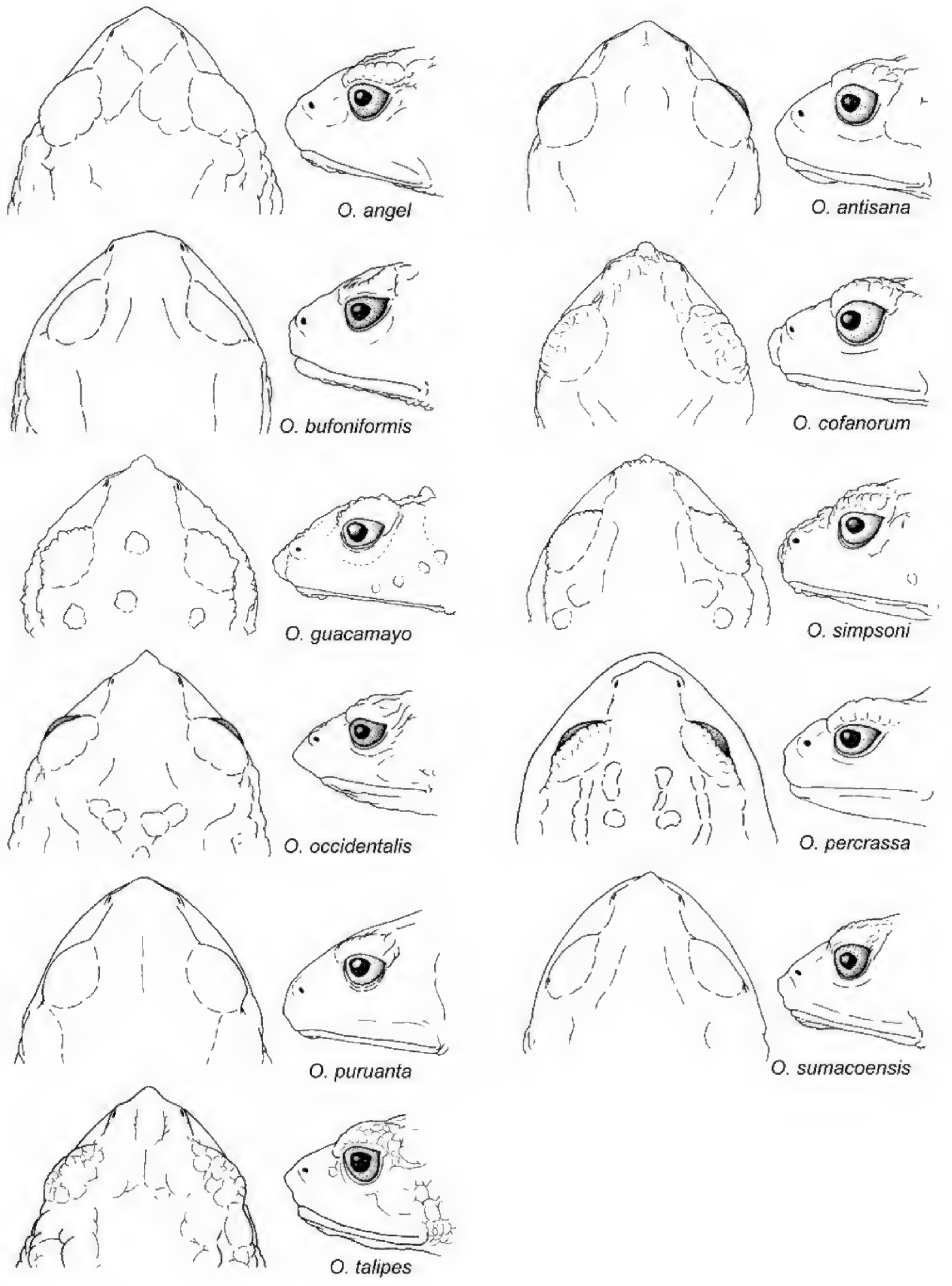

Figure 11. Head shape in dorsal and lateral views of *Osornophryne* females. Illustrated species are: *O. angel,* QCAZ 43560; *O. antisana,* QCAZ 48221; *O. bufoniformis,* QCAZ 40122; *O. cofanorum,* DH-MECN 6194; *O. guacamayo,* QCAZ 26047; *O. simpsoni,* DH-MECN 5260; *O. occidentalis,* QCAZ 43498; *O. percrassa,* ICN 319; *O. puruanta,* QCAZ 11471; *O. sumacoensis,* QCAZ 41244; *O. talipes,* EPN 2823. Not drawn at scale.

7	Males and females large (in males, SVL > 23.5 mm; in females, SVL > 40 mm); males and females with a continuous dorsolateral ridges, and acuminate snout in dorsal view (Figs 10, 11) **8**
–	Males and females small (in males, SVL < 19.0 mm; in females, SVL < 30 mm). Males and females with discontinuous dorsalateral ridges..... ***O. antisana***
8	Males and females with prominent dorsolateral, occipital, and pelvic ridges.. ..... ***O. talipes***
–	Females with comparatively lower dorsolateral, occipital, and pelvic ridges (males unknown) ..... ***O. puruanta***
9	Females with yellow, orange, or white venter in life..... **10**
–	Females with blue to silver venter in life; males with a yellow to orange papillae at tip of snout (Figs 10, 11) ..... ***O. sumacoensis***
10	Females with yellow to orange venter in life; males and females lacking dorsolateral ridges ..... ***O. percrassa***
–	Females with yellow to white venter; males and females with clearly defined dorsolateral ridges ..... ***O. occidentalis***

Acknowledgments

This article was greatly improved by comments from Linda Trueb, Franco Andreone and Andrew Gluesenkamp. Initial field work has possible thanks to the project "Evaluación de la Herpetofauna de las Reservas Biológicas de la Fundación Ecominga. Cuenca Alta del Río Pastaza. Ecuador", executed by the Museo Ecuatoriano de Ciencias Naturales and funded by Fundación Jocotoco and Fundación Ecominga. Research was supported by the projects "Inventario y Caracterización Genética y Morfológica de la Diversidad de Anfibios, Aves y Reptiles de los Andes del Ecuador" and "Diversidad Críptica de los Géneros *Pristimantis, Osornophryne* e *Hypsiboas,*" granted by the Secretaría Nacional de Ciencia y Tecnología del Ecuador (PIC-08-0000470) and the Pontificia Universidad Católica del Ecuador, respectively. Universidad Tecnológica Indoamérica supported the final phase of this investigation. For access to collection specimens, we thank the Museo Ecuatoriano de Ciencias Naturales, Museo de Zoología of the Pontificia Universidad Católica del Ecuador, and the Museo de Zoología de la Escuela Politécnica Nacional. Research was conducted under collection permit No. 021–08 IC-FAU-DNBAPVS/MA, issued by Ministerio del Ambiente del Ecuador. Fieldwork at Reserva Zuñac was possible thanks to the collaboration of Lou Jost, Francisco Sornoza M., Rocío and Javier Robayo. MYM thanks Miguél Urgiles, Juan P. Reyes Puig and Andrés Laguna for assistance during field work, and Mauro Yánez C., Joaquín Yánez C., and Alejandra Bejarano for their continuous support. Special thanks go to Elicio Tapia, who found many of the specimens herein reported, Luis A. Coloma and Eduardo Toral for the photographs shown in Figures 2 and 3, and Diego Paucar, who rendered most of the figures shown in this article (Figs 4–8, Figs 10–11).

References

Alfaro ME, Zoller S, Lutzoni F (2003) Bayes or bootstrap? A simulation study comparing the performance of Bayesian Markov chain Monte Carlo sampling and bootstrapping in assessing phylogenetic confidence. Molecular Biology and Evolution 20: 255–266. doi:10.1093/molbev/msg028

Bocxlaer IV, Loader SP, Roelants K, Biju SD, Menegon M, Bossuyt F (2010) Gradual adaptation toward a range-expansion phenotype initiated the global radiation of toads. Science 327: 679–682. doi:10.1126/science.1181707

Cannatella DC (1986) A new genus of bufonid (Anura) from South America, and phylogenetic relationships of the neotropical genera. Herpetologica 42: 197–205.

Cisneros-Heredia DF, Gleusenkamp AGG (2010) A new Andean toad of the genus *Osornophryne* (Amphibia: Anura: Bufonidae) from northwestern Ecuador, with taxonomic remarks on the genus. Avances en Ciencias e Ingenierías 2: B64–B73.

Coloma LA (1997) Morphology, systematics, and phylogenetic relationships among frogsof the genus Atelopus (Anura: Bufonidae). Unpublished PhD dissertation, The University of Kansas, Lawrence.

Duellman WE, Trueb L (1994) Biology of Amphibians. The Johns Hopkins University Press, USA.

Erixon P, Svennblad B, Britton T, Oxelman, B (2003) Reliability of Bayesian posterior probabilities and bootstrap frequencies in phylogenetics. Systems Biology 52: 665–673. doi:10.1080/10635150390235485

Fabrezi M (1992) El carpo de los anuros. Alytes 10: 1–29.

Fabrezi M (1993) The anuran tarsus. Alytes 11: 47–63.

Fabrezi M, Alberch P (1996) The carpal elements of anurans. Herpetologica 52: 188–204.

Gluesenkamp AG (1995) A new species of *Osornophryne* (Anura: Bufonidae) from Volcán Sumaco, Ecuador with notes on other members of the genus. Herpetologica 51: 268–279.

Gluesenkamp AG (2001) Development mode and adult morphology in bufonid frogs: A comparative analysis of correlated traits. PhD thesis, Texas University, Austin.

Gluesenkamp AG, Guayasamin JM (2008) A new species of *Osornophryne* (Anura: Bufonidae) from the Andean highlands of northern Ecuador. Zootaxa 1828: 18–28.

Goebel AM, Donnelly JM, Atz ME (1999) PCR primers and amplification methods for 12S ribosomal DNA, the control region, cytochrome oxidase I, and cytochrome b in bufonids and other frogs, and an overview of PCR primers which have amplified DNA in amphibians successfully. Molecular Phylogenetics and Evolution 11: 163–199. doi:10.1006/mpev.1998.0538

Graybeal A (1997) Phylogenetic relationships of bufonid frogs and test of alternate macroevolutionary hypotheses characterizing their radiation. Zoological Journal of the Linnean Society 119: 297–338. doi:10.1111/j.1096-3642.1997.tb00139.x

Hillis DM, Bull JJ (1993) An empirical test of bootstrapping as a method for assessing confidence in phylogenetic analysis. Systematic Biology 42: 182–192.

Hoogmoed MS (1987) New *Osornophryne* (Amphibia: Anura: Bufonidae) from the Pacific slopes of the Andes in Ecuador. Zoologische MEdedelingen 61: 209–242.

Larkin MA, Blackshields G, Brown NP, Chenna R, McGettigan PA, McWilliam H, Valentin F, Wallace IM, Wilm A, Lopez R, Thompson JD, Gibson TJ, Higgins DG

(2007) Clustal W and Clustal X version 2.0. Bioinformatics 23: 2947–2948. doi:10.1093/bioinformatics/btm404

Maddison WP, Maddison DR (2009) Mesquite: a modeular system for evolutionary analysis ver 2.71. http://mesquiteproject.org.

Mueses-Cisneros JJ, Yánez-Muñoz MH, Guayasamin JM (2010) Una nueva especie de sapo del género *Osornophryne* (Anura: Bufonidae) de las estribaciones amazónicas de los Andes de Ecuador. Papéis Avulsos de Zoologia 50: 269–279.

Padial JM, Castroviejo-Fisher S, Köhler J, Vilà C, Chaparro JC, De la Riva I (2009) Deciphering the products of evolution at the species level: the need for an integrative taxonomy. Zoologica Scripta 38: 431–447. doi:10.1111/j.1463-6409.2008.00381.x

Peracca MG (1904) Rettili ed amfibii in viaggio del Dr. Enrico Festa nell" Ecuador e regioni vicine. Bolletino dei Musei di Zoologia ed Anatomia Comparata della Universitá di Torino 19: 1–41.

Posada D (2008) jModelTest: Phylogenetic Model Averaging. Molecular Biology and Evolution 25: 1253–1256. doi:10.1093/molbev/msn083

Pramuk JB (2006) Phylogeny of South American *Bufo* (Anura: Bufonidae) inferred from combined evidence. Zoological Journal of the Linnean Society 146: 407–452. doi:10.1111/j.1096-3642.2006.00212.x

Rambaut A, Drummond AJ (2007) Tracer v1.4. http://beast.bio.ed.ac.uk/Tracer

Ronquist F, Huelsenbeck JP (2003) MrBayes 3: Bayesian phylogenetic inference under mixed models. Bioinformatics 19: 1572–1574. doi:10.1093/bioinformatics/btg180

Ruiz-Carranza PM, Hernández-Camacho JA (1976) *Osornophryne* género nuevo de anfibios bufónidos de Colombia y Ecuador. Caldasia 11: 93–148.

Shubin N, Alberch P (1986) A morphogenetic approach on the origin and basic organization of the tetrapod limb. In: Hecht M, Wallace B, Prance G (Eds) Evolutionary Biology. Plenum Press, New York, 319–387.

Simpson GG (1961) Principles of Animal Taxonomy. Columbia University Press, New York.

Swofford DL (2009) Phylogenetic Analysis Using Parsimony (*and Other Methods) ver 4.0a109. Sinauer Associates, Sunderland, Massachusetts.

Taylor WR, Van Dyke GC (1985) Revised procedures for staining and clearing small fishes and other vertebrates for bone and cartilage study. Cybium 9: 107–119.

Trueb L (1973) Bones, frogs, and evolution. In: Vial JL (Ed) *Evolutionary Biology of the Anurans.* University of Missouri Press, Columbia, 79–108.

Trueb L (1993) Patterns of cranial diversity among the Lissamphibia. In: Hanken J, Hall BK (Eds) The Skull: Patterns of Structural and Systematic Diversity, Vol. 2. Chicago University Press, Chicago, 255–343.

Wiens JJ (2004) Speciation and ecology revisited: phylogenetic niche conservatism and the origin of species. Evolution 58: 193–197.

Wiley EO (1978) The evolutionary species concept reconsidered. Systematic Zoology 27: 17–26. doi:10.2307/2412809

Yánez-Muñoz MH, Altamirano-Benavides M, Cisneros-Heredia DF, Gluesenkamp AGG (2010) Nueva especie de sapo andino del género *Osornophryne* (Amphibia: Bufonidae) del norte de Ecuador, con notas sobre la diversidad del género en Colombia. Avances en Ciencias e Ingenierías 2: B46–B53.

Zwickl DJ (2006) Genetic algorithm approaches for the phylogenetic analysis of large biological sequence datasets under the maximum likelihood criterion. PhD thesis, Texas University, Austin.

Appendix I: Examined Specimens

Osornophryne angel: Carchi: El Voladero (0°41'15"N, 77°52'46"W), DH-MECN 4617, 4606, 4629–30, 4626, 6079, QCAZ 40030–31, 40040, 40043–49.

Osornophryne antisana: Napo: Oyacachi (0°10'34"S, 78°0.6'50"W, 3913 m) QCAZ 40172, 40174; Salvefaccha (0°13'54"S, 78°0.1'01"W, 3900 m) EPN 8937. Tungurahua: Llanganates (1°15'57"S, 78°26'45"W, 3600 m), QCAZ 515, 46282, 48231, 46207, 46204–5, 48230, 48487, 48233–36, 48222, 48215, 48217, 48213, 46212.

Osornophryne bufoniformis: Carchi: Huaca (77°46'11"N, 0°40'15"W, 3780 m) QCAZ 45082–4, 45080–81, 43351; El Chamizo QCAZ 14597–98; Tulcán-Maldonado (0°47'31"N, 77°54'25"W, 3817 m) QCAZ 735, 9316–17. Sucumbios: El Playón de San Francisco (00°36'44"N, 77°40'13"W, 3400–4100 m), DH-MECN 6067–70, 6073, 6079, 6082; La Bonita (00°29”19"N, 77°35”11.4"W, 2614 m) QCAZ 46640–43; Santa Bárbara (0°38'29.47"N, 77°31'18.55"W, 2700 m), QCAZ 40003, 40122, 14080–81, 40118–19.

Osornophryne cofanorum: Sucumbios: La Bonita (0°29'19"N, 77°35'11"W, 2614 m), DH-MECN 6192, 6194, 6205, 6214, 6219, 6232, 6237, 6243, 6250, 6296–97, 6300, 6303–04, 6315, 6325, 6328, 6334, 6337, 6339.

Osornophryne guacamayo: Napo: Cordillera de los Guacamayos (0°37'26.5"S, 77°50'27.09"W, 2238 m), QCAZ 3266, 4889, 9894, 12245, 12249, 13260, 12240, 13259, 26047, 26049, 39081, 33197, 10457, 40106, 40111, 10465, 12241, EPN 6822, 6821, 7438, 7806; Oyacachi (0°15'25"S, 77°57'53"W, 2253 m), QCAZ 40158, 40169, 40138, 40143, 40160, 40148, 40137; Volcán Sumaco (0°34'11"S, 77°35'39"W, 2479 m), QCAZ 41211, 41206, 41210, 41194, 41207, 41229, 41196, 41223, 41203, 41190, 43378, 43370, 43377, 43551–54, 43557, 43550, 43557–59. Sucumbios: Santa Bárbara (0°33'51.4"N, 77°32'50"W, 2388 m), QCAZ 46661.

Osornophryne occidentalis: Carchi: Chilma Bajo (0°51'50"N, 78°4'01"W, 2237 m), QCAZ 40028. Imbabura: Rosario (0°27'29"N, 78°32'50"W, 2296 m) QCAZ 36894, 43498, 43649, 43647, 10141, 43652, 43529, 43650, 43646, 43651, 43653. Pichincha: Guarumos (00°02”S, 78°39”W, 2550–2600 m) EPN 1239.

Osornophryne puruanta: Imbabura: Laguna de Puruanta (00°12'N, 77°57'W, 3000–3500 m) QCAZ 11471, 7685. Pichincha: Laguna de San Marcos (0°7'36"N, 78°15'22"W, 3834 m), EPN7081–83, QCAZ 13271.

Osornophryne sumacoensis: Napo: Volcán Sumaco (0°34'11"S, 77°35'39"W, 2479 m), QCAZ 41247–50, 41243–54, 41233–34, 43379, 4574.